Research Article | Vol. 30, No. 11 / 23 May 2022 / Optics Express 19805
Optics EXPRESS

All-silica optical fiber bonding

PAWEL MANIEWSKI,* MICHAEL FOKINE, AND FREDRIK LAURELL

Laser physics group, School of Engineering Science, KTH Royal Institute of Technology, Stockholm, Sweden
pawelma@kth.se

Abstract: In this work, we demonstrate a spot-welding method for fabrication of all-silica fiber components. A CO_2 laser was used to locally sinter sub-micron silica powders, enabling rigid bonding of optical fiber to glass substrates. The bonding was achieved without inducing any fiber transmission losses. The components showed no sign of deterioration or structural change when heated up to 1100 °C. These single material assemblies are therefore well suited for use in harsh environments where high stability and robustness is required.

1. Introduction

Assembly and mounting of silica based optical fibers used in harsh conditions, such as corrosive environment, high temperature sensing or high-power laser applications is a challenge when it comes to bonding materials [1,2]. Common solutions used for optical communication, sensing and medical systems are mostly based on fibers mounted in ferrules or silicon V-groove chips using polymer adhesives, metal soldering, or laser welding [3–11]. Device failure is typically linked to difference in thermal expansion coefficient, polymer degradation, uneven curing, or low melting temperature of the adhesive [5]. The ideal case would be a single material structure thereby circumventing problems arising from the mismatch in material properties of substrate, fiber, and bonding material. For optical fibers this would mean direct bonding of the fibers to a silica substrate. Direct fusion of optical fibers, using for example laser heating or plasma discharge, may however lead to deformation of the fibers with subsequent loss in performance.

In this work, we demonstrate spot-welding of optical fibers using CO_2 laser radiation in combination with glass powder injection. The resulting formation of silica beads form a strong permanent bond with high-temperature resistance. By placing the beads at the junction between fiber and substrate, damage to the fiber can be avoided maintaining the optical properties, while providing sufficient mechanical bonding. The mechanical integrity of the spot-welded fibers was maintained even after heat-treatment up to 1100 °C.

2. Design and methods

2.1. Experimental setup and preparation

The experimental setup used in this work was previously developed for use in additive manufacturing of transparent silica glass using sub-micron powders [12,13]. Using a long wavelength laser together with sub-micron silica powder reduces energy scattering and minimizes substrate shadowing [14] resulting in homogeneous substrate irradiation and stable processing temperature.

The setup is shown in Fig. 1. The CO_2 laser (ULR-50, Universal Laser Systems) beam was focused onto the substrate using a ZnSe spherical lens with a focal length of 40 mm. The lens was integrated into the print head which included three powder nozzles. It was mounted onto a motorized stage to allow for adjustment of the spot size on the sample. The nozzles were aligned so that the powder jets intersected with the laser beam at the substrate. Substrate translation perpendicular to the laser beam was performed using CNC stages. A computer-controlled mechanical shutter was used to control the deposited energy during powder sintering. The

#457358 https://doi.org/10.1364/OE.457358
Journal © 2022 Received 1 Mar 2022; revised 13 Apr 2022; accepted 13 Apr 2022; published 19 May 2022

Optics EXPRESS

laser exposure conditions were optimized experimentally to obtain sufficient sintering for strong fiber-to-substrate bonding, while at the same time avoiding deformation of the fiber.

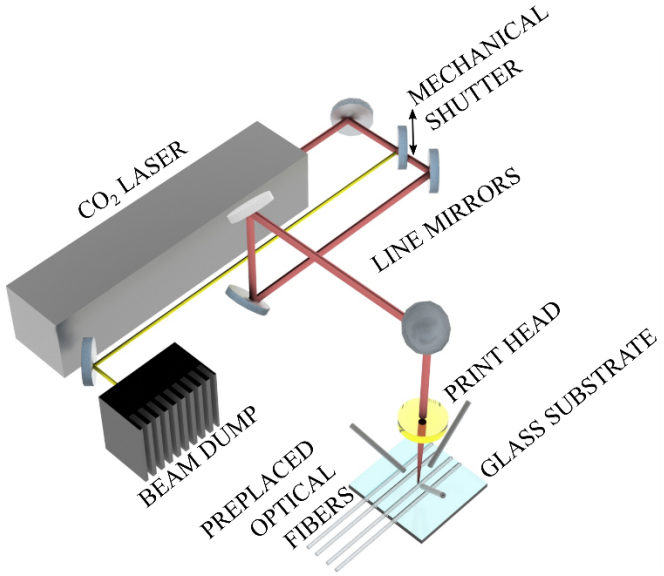

Fig. 1. Sketch of the experimental setup for fiber welding.

2.2. *Spot-welding*

In these experiments, we welded standard silica fibers (SMF-28, Corning Inc.), with the polymer coating removed, onto the 1 mm thick quartz glass substrates ($25 \times 25 \times 1$ mm^3, PlanOptik AG). Figure 2 shows the main fabrication steps. A high-speed rotational saw (Disco Corp.) equipped with a diamond blade was used to cut the guiding trenches in the substrates for placement of the fibers. Two welding configurations were investigated using different trench width. In the first configuration 100 µm wide trenches were cut into the substrate. The 125 µm diameter fibers therefore rested on two contact points, similarly to how typical silicon V-grooves are used [3–5]. In the second configuration, 200 µm wide and 200 µm deep trenches were made. In this case the fibers were placed at the bottom of the trenches being embedded under the surface of the substrate. The edge-to-edge separation between trenches was 200 µm. Prior to spot-welding the fibers were temporarily fixed in the trenches using wax at each end of the substrate (see Fig. 2(b)). During welding, the substrate was stationary with the powder sintered into a single weld bead. Each bead was formed by exposing a 1.2 mm diameter laser spot having a power of P = 14.5 W for a duration of 0.1 s. Simultaneously fumed silica powder (Alpha Aesar, feed rate, 0.5 g/min) was injected using the three powder jets. The welding parameters were developed experimentally. Each fiber was bonded to the substrate using 40 consecutive weld points, 20 on each side of the fiber (Fig. 2(c)). Once the welding was complete the wax was removed from the assembly by ultrasonic cleaning using toluene followed by acetone, and methanol. Finally, a flat parallel end-face was obtained by dicing the assembly perpendicular to the fibers using the high-speed dicing saw, see Fig. 2(d). By using the high-speed dicing saw, and optimized dicing parameters, smooth end-faces with high surface quality were achieved [15–17]. This was confirmed by optical inspection of the cross-section.

Optics EXPRESS

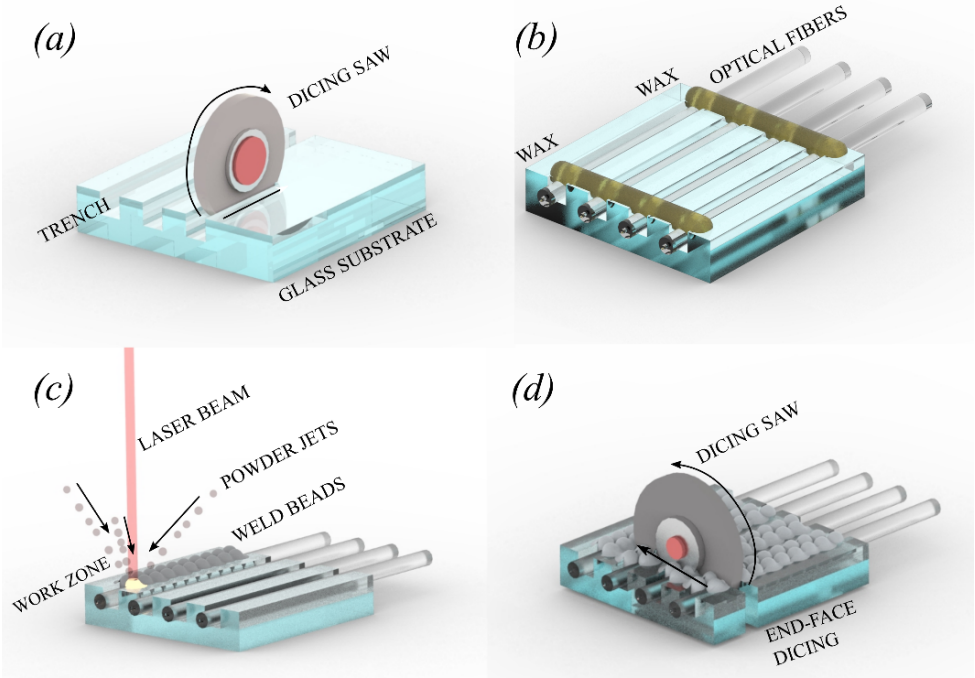

Fig. 2. Processing steps including: (a) cutting of the trenches, (b) fiber mounting, (c) powder sintering, and (d) end-face dicing.

2.3. Sample evaluation

Three tests were performed to evaluate the assembly. To check if the spot-welding affected the throughput of light a fiber-coupled laser diode at $\lambda = 1550$ nm was launched through the fiber. The transmitted signal was then measured during the welding process to assess heat induced losses. The tensile strength of the welded fibers was tested by fixing the assemblies on an aluminum breadboard and pulling the fibers with a tension sensor (Hans Schmidt, FSL-500). To evaluate the mechanical stability of these single-material assemblies, samples were heat treated up to 1100 °C for a duration of several minutes with subsequent visual inspection to identify any delamination, detachment, or cracks.

3. Experimental results

First, the assemblies with 100 µm trenches were investigated. The weld bead layout used is shown in Fig. 3(a). It has been optimized experimentally to achieve a layer of weld beads that fully cover the fiber. Welding with sparser layout was less rigid, while denser layout did not improve bonding strength. The diameter of a single weld bead corresponds to the laser-induced hot zone, which was approximately 1.2 mm. The consecutive weld beads were overlapping each other, creating an undulating, printed layer on top of the substrate with the fiber underneath. After end-face dicing, the cladding of the fiber was found chipped however, the fiber's core was undamaged. The test sample is shown in the photograph in Fig. 3(b).

The second type of assemblies, with the fibers embedded in the 200 µm wide trenches, is sketched in Fig. 4(a), while Fig. 4(b, c) shows photographs of the end-face and the corresponding top view of such an assembly with three parallel fibers.

During spot-welding, the transmitted power was measured in-situ on each of the three fibers (see Fig. 4(a)). The transmitted signal was normalized to the initial power level as shown in Fig. 5.

Optics EXPRESS

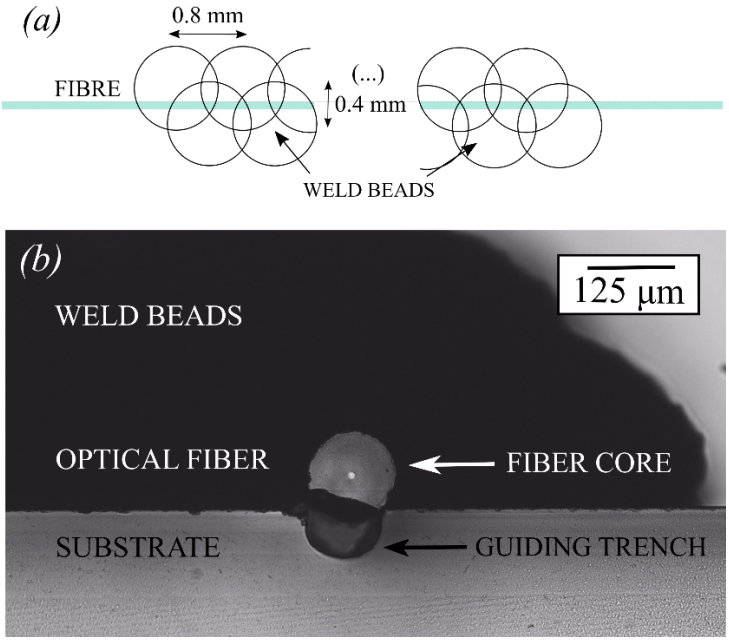

Fig. 3. Sketch (a) of weld bead pattern used in the experiments as seen from the top, and (b) photograph of a typical end-face of bonded fiber. Bottom-illumination was used.

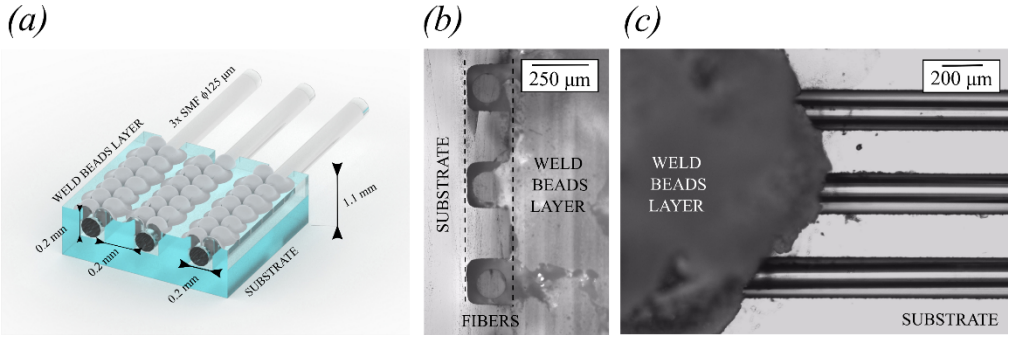

Fig. 4. Schematic (a) of the test assembly, and (b) photographs of the diced end-face (top-illumination), and (c) a top view of it.

Optics EXPRESS

Data for the three measurements are offset for clarity. The induced loss during spot-welding was up to ≈ 4%. After welding the transmitted signal returned to its initial value within measurement resolution.

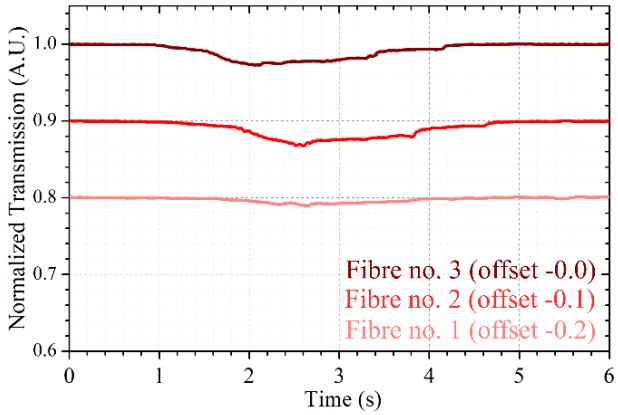

Fig. 5. Normalized transmission through three subsequent fibers during spot-welding (offset for clarity).

During the tensile strength test all assemblies withstood an axial load (pulling along the axis of the fiber) exceeding 1.50 N. The failure points were all located at the edge of the first weld bead, with the remaining fiber still being welded to the substrate.

4. Discussion

Although transparent glass can be printed using this technique [12], the weld beads made in this work were non-transparent with a partly sintered and porous structure. Printing of fully sintered glass requires higher energy, and it could risk damaging the fiber. In this work we focused on obtaining a sufficiently strong bond while maintaining the transmission properties of the fibers. A small reduction of transmitted power was measured during spot-welding, see Fig. 5. This effect is ascribed to large temperature gradients across the fiber, which are typical for CO_2 laser processing [18,19]. Once the welding was complete and the assemblies had cooled down, the transmission returned to its initial value.

The tensile strength test showed that the bonding to the substrate was strong, and the failure point was always located at the outer edge of the weld beads corresponding to the maximum stress point. Any angular misalignment of the pulling force would further increase the risk of cleaving the fiber.

A single material structure, which is demonstrated here, should have superior thermal stability. To evaluate the robustness the assembly was placed in a furnace and the temperature was increased up to 1100 °C. Even after processing at these extreme temperatures no structural change of the assemblies was observed, and the weld beads were intact. The test performed on our samples at 1100 °C should be viewed as an extreme form of accelerated ageing, and not an upper limit of use.

By comparing the two welding configurations we found that the two-point contact configuration (100 µm trench) provided higher accuracy in fiber positioning, but it was more prone to damage. As there was an air gap below the fiber, i.e., no bonding, this unsupported section tended to chip off during the final end-face dicing, see Fig. 3. Potentially this can lead to significant damage to the fiber and corresponding performance decrease, depending on the amount of chipping. The embedded fiber configuration (200 µm trench) resulted in a more robust bonding without chipping when diced, but with a lower precision in positioning.

Optics EXPRESS

The trench size was determined by the width of the diamond blade. In this work we were limited to blades with widths of 100 µm and 200 µm. To improve the positioning in the embedded configuration a trench width slightly larger than the diameter of the fiber should be used.

5. Conclusion

In this work a novel method for bonding of optical fibers onto glass substrates using silica powder has been demonstrated, representing a single material assembly suitable for use in harsh environments where high stability and robustness is required.

Spot-welding was performed using a CO_2 laser to locally sinter sub-micron silica powders, resulting in strong bonding between fiber and substrate. By using suitable laser welding parameters bonding was achieved without any induced fiber transmission losses. The test assemblies showed high stability and robustness without any structural change even when heated to temperatures as high as 1100 °C.

Funding. Knut och Alice Wallenbergs Stiftelse (2016.0104); Stiftelsen för Strategisk Forskning (GMT14-0071, RMA150135).

Disclosures. The authors declare no conflicts of interest.

Data availability. Data underlying the results presented in this paper are not publicly available at this time but may be obtained from the authors upon reasonable request.

References

1. M. A. Uddin, M. Y. Ali, and H. P. Chan, "Materials and fabrication issues of optical fiber array," Rev. Adv. Mater. **21**(2), 155–164 (2009).
2. W. Wang, W. Wu, S. Wu, Y. Li, C. Huang, X. Tian, X. Fei, and J. Huang, "Adhesive-free bonding homogenous fused-silica Fabry–Perot optical fiber low pressure sensor in harsh environments by CO_2 laser welding," Opt. Commun. **435**, 97–101 (2019).
3. A. Velazquez-Benitez, J. E. Antonio-Lopez, J. C. Alvarado-Zacarias, N. K. Fontaine, R. Ryf, H. Chen, J. A. Hernández-Cordero, P. Sillard, C. M. Okonkwo, S. G. Leon-Saval, and R. Amezcua-Correa, "Scaling photonic lanterns for space-division multiplexing," Sci. Rep. **8**(1), 8897 (2018).
4. E. Murphy, T. Rice, L. McCaughan, G. Harvey, and P. Read, "Permanent attachment of single-mode fiber arrays to waveguides," J. Lightwave Technol. **3**(4), 795–799 (1985).
5. J. A. Duan and Y. Zheng, "Experimental Study of the Packaging Failure for Optical Fiber Arrays," Adv. Mat. Res. **295-297**, 1594–1599 (2011).
6. M. Shaw, R. Galeotti, and G. Coppo, "Method of fixing an optical fibre in a laser package," *Proc. 51st Electronic Components and Technology Conference (Cat. No.01CH37220)*, 1441–1446, (2001).
7. A. Janta-Polczynski, E. Cyr, R. Langlois, P. Fortier, Y. Taira, N. Boyer, and T. Barwicz, "Solder-reflowable single-mode fiber array photonics assembly in high-throughput manufacturing facilities," Proc. SPIE **10924**, 32 (2019).
8. J. H. C. van Zantvoort, S. G. L. Plukker, E. C. A. Dekkers, G. D. Khoe, A. M. J. Koonen, and H. de Waardt, "Laser supported fibre array alignment with individual fibre fine positioning," Proc. Electron. Compon. Technol. Conf. **1**, 266–271 (2005).
9. K. W. Lam, M. Uddin, and H. P. Chan, "Reliability of adhesive bonded optical fiber array for photonic packaging," J. Optoelectron. Adv. Mater. **10**, 67811N (2008).
10. N. Murata and K. Nakamura, "UV-Curable Adhesives for Optical Communications," J. Adhes **35**(4), 251–267 (1991).
11. M.R. Finardi, C.A. Finardi, R.R. Panepucci, J. Miyoshi, E. Zambotti, and L.T. Zanvettor, "Development of optical fiber arrays based on silicon V-Grooves," *SBMO/IEEE MTT-S International Microwave and Optoelectronics Conference (IMOC)*, 1–4 (2015).
12. P. Maniewski, F. Laurell, and M. Fokine, "Laser cladding of transparent fused silica glass using sub-micron powder," Opt. Mater. Express **11**(9), 3056–3070 (2021).
13. P. Maniewski, F. Laurell, and M. Fokine, "Quill-free additive manufacturing of fused silica glass," Opt. Mater. Express **12**(4), 1480–1490 (2022).
14. P. Maniewski, F. Laurell, and M. Fokine, "Reduction of shadowing effect during laser cladding of fused silica glass using sub-micron powders," Proc. SPIE **11677**, 34 (2021).
15. T. G. Bifano, T. A. Dow, and R. O. Scattergood, "Ductile-Regime Grinding: A New Technology for Machining Brittle Materials," ASME. J. Eng. Ind. **113**(2), 184–189 (1991).
16. H. E. Parker, S. Sengupta, A. V. Harish, R. G. Soares, H. N. Joensson, W. Margulis, A. Russom, and F. Laurell, "A Lab-in-a-Fiber optofluidic device using droplet microfluidics and laser-induced fluorescence for virus detection," Sci. Rep. **12**(1), 3539 (2022).
17. E. Brinksmeier, Y. Mutlugünes, F. Klocke, J. C. Aurich, P. Shore, and H. Ohmori, "Ultra-precision grinding," CIRP Ann. **59**(2), 652–671 (2010).

Optics EXPRESS

18. W. Guo, P. Holmberg, F. Laurell, and M. Fokine, "Fabrication of long-period fiber gratings through periodic ablation using a focused CO_2-laser beam," Opt. Mater. Express **5**(11), 2702–2714 (2015).
19. J. M. P. Coelho, M. Nespereira, M. Abreu, and J. Rebordão, "3D Finite Element Model for Writing Long-Period Fiber Gratings by CO_2 Laser Radiation," Sensors **13**(8), 10333–10347 (2013).